Synthesis and Characterization of the Paramagnetic $[Ag_{13}Fe_8(CO)_{32}]^{4-}$ Tetraanion: A Cuboctahedral Ag_{13} Cluster Stabilized by $Fe(CO)_4$ Groups Behaving as Four-Electron Donors

Vincenzo G. Albano,[†] Loris Grossi,[‡] Giuliano Longoni,*[,§] Magda Monari,[†] Suzanne Mulley,[§] and Angelo Sironi[⊥]

Contribution from the Dipartimento di Chimica "G. Ciamician", via F. Selmi 2, 40126 Bologna, Italy, Dipartimento di Chimica Organica, viale Risorgimento 4, 40136 Bologna, Italy, Dipartimento di Chimica Fisica ed Inorganica, viale Risorgimento 4, 40136 Bologna, Italy, Istituto di Chimica Strutturistica Inorganica, via Venezian 21, 20133 Milano, Italy.
Received October 21, 1991

Abstract: The new $[Ag_{13}Fe_8(CO)_{32}]^{4-}$ paramagnetic cluster anion has been obtained in a mixture with other yet uncharacterized products from the reaction of $Na_2[Fe(CO)_4]\cdot x$THF with ca. 1.5 equiv of $AgBF_4$ or $AgNO_3$ in tetrahydrofuran and acetonitrile solution, respectively. It has been separated from the mixture via differential solubility of the tetrasubstituted ammonium or phosphonium salts and isolated in a crystalline state as $[NMe_3CH_2Ph]^+$ and $[N(PPh_3)_2]^+$ salts. The structure has been determined by X-ray diffraction studies on a crystal of the latter salt: monoclinic, space group $P2_1/n$, a = 18.321 (2) Å, b = 22.429 (3) Å, c = 22.150 (1) Å, β = 92.24 (2)°, Z = 2, R = 0.0410. The molecular structure of the anion consists of an Ag_{13} centered cuboctahedron capped on all the triangular faces by $Fe(CO)_4$ groups displaying C_{3v} symmetry; the eight iron atoms describe a distorted cube. The idealized molecular symmetry is O_h. The unpaired electron present in $[Ag_{13}Fe_8(CO)_{32}]^{4-}$ is strongly coupled with the unique interstitial silver atom and loosely coupled with the 12 peripheral silvers. The electron count of the cluster, having extra nine electrons with respect to the number predicted by most theories, as well as the hyperfine structure of the ESR spectrum, have both been interpreted on the basis of extended Huckel molecular orbital calculations.

Introduction

While investigating the oxidation products of $[Fe_4P(CO)_{13}H_{3-n}]^{n-}$ (n = 2, 3)[1] and $[Fe_3In(CO)_{12}]^{3-}$[2] with silver salts, we detected by ESR the formation in solution of trace amounts of an unknown paramagnetic species. This species displayed a complicated signal probably consisting of two doublets of multiplets; such a hyperfine structure was suggestive of a weaker interaction of the unpaired electron with several equivalent nuclei and stronger coupling with one or two nuclei unequivalent or different from the former. Since the only spin-active element common to both reactions was silver, whose natural isotopic composition is ^{107}Ag ($S = {}^1/_2$; 51%) and ^{109}Ag ($S = {}^1/_2$; 49%), it was consequent to attribute the presence of the above ESR signal to the formation of a paramagnetic silver cluster, probably related to the previously reported Cu-Fe bimetallic clusters, $[Cu_6Fe_4(CO)_{16}]^{2-}$, $[Cu_5Fe_4(CO)_{16}]^{3-}$, and $[Cu_3Fe_3(CO)_{12}]^{3-}$.[3,4] Several polynuclear organometallic[5] and thiolate silver compounds[6] are known, whereas to our knowledge the only clusters containing a silver core so far reported are bimetallic, e.g., $Ag_6Fe_3(CO)_{12}\{(PPh_2)_3CH\}$,[7] $[Ag_3Rh_3H_9\{(PPh_2CH_2)_3CCH_3\}_3]^{3+}$,[8] $Ag_3M_3(CO)_{12}(dmpe)_3$ (M = Nb, Ta),[9] and the remarkable series of Ag-Au bimetallic supraclusters characterized by B. K. Teo.[10-15]

Conversely, bare silver clusters trapped in noble gas or other inert matrices[16-19] or in zeolites[20,21] have been thoroughly investigated in view of their obvious relationship with silver clusters trapped in a silver halide matrix, which are at the origin of the formation of latent images on photographic films.[22]

The above observations and the expected ductility of $Fe(CO)_4$ fragments as ligands, prompted the investigation of the reaction of iron carbonyl anionic species with silver salts. We report here our first results consisting of the synthesis and characterization of the paramagnetic $[Ag_{13}Fe_8(CO)_{32}]^{4-}$ tetraanion.

Results and Discussion

1. Synthesis and Spectroscopic Characterization of $[Ag_{13}Fe_8(CO)_{32}]^{4-}$. The progressive addition up to a ca. 1.8 molar ratio of $AgBF_4$ or $AgNO_3$ with respect to $Na_2[Fe(CO)_4]\cdot x$THF in tetrahydrofuran (THF) or acetonitrile solution yields a series of new carbonyl species showing infrared absorptions of increasingly higher frequency (up to ca. 2000 cm^{-1}). Most of these absorptions do not match those of the known iron carbonyl anions with greater molecular complexity, e.g., $[Fe_2(CO)_8]^{2-}$, $[Fe_3(CO))_{11}]^{2-}$, etc.,[23] which could be expected to arise from simple oxidation of $[Fe(CO)_4]^{2-}$.[24] ESR monitoring of the above reaction shows the formation of a paramagnetic species, displaying ESR features similar to those displayed by the byproduct of the oxidation of $[Fe_4P(CO)_{13}]^{3-}$[1] as well as $[Fe_3In(CO)_{12}]^{3-}$[2] with silver ions. Its concentration generally reaches a maximum after addition of 1.5-1.7 equiv of Ag^+ per mol of $[Fe(CO)_4]^{2-}$. At this stage, the infrared spectrum of the solution shows the strongest carbonyl

(1) Albano, V. G.; Canè, M.; Iapalucci, M. C.; Longoni, G.; Monari, M. *J. Organomet. Chem.* **1991**, *407*, C9.
(2) Canè, M.; Iapalucci, M. C.; Longoni, G.; Demartin, F.; Grossi, L. *Materials Chem. Phys.* **1991**, *29*, 395.
(3) Doyle, G.; Eriksen, K. A.; Van Engen, D. *J. Am. Chem. Soc.* **1986**, *108*, 445.
(4) Doyle, G.; Eriksen, K. A.; Van Engen, D. *J. Am. Chem. Soc.* **1985**, *107*, 7914.
(5) Noltes, J. G.; van Koten, G. In *Comprehensive Organometallic Chemistry*; Wilkinson, G., Stone, F. G. A., Abel, E. W., Eds.; Pergamon Press: Oxford, Vol. 2, p 709.
(6) Dance, I. G.; Fitzpatrick, L. J.; Craig, D. G.; Scudder, M. L. *Inorg. Chem.* **1989**, *28*, 1853 and references therein.
(7) Briant, C. E.; Smith, R. G.; Mingos, D. P. M. *J. Chem. Soc., Chem. Commun.* **1984**, 586.
(8) Bachechi, F.; Ott, J.; Venanzi, L. M. *J. Am. Chem. Soc.* **1985**, *107*, 1760.
(9) Calderazzo, F.; Pampaloni, G.; Englert, U.; Strahle, J. *J. Organomet. Chem.* **1990**, *383*, 45.
(10) Teo, B. K.; Shi, X.; Zhang, H. *J. Am. Chem. Soc.* **1991**, *113*, 4329.
(11) Teo, B. K.; Keating, K. *J. Am. Chem. Soc.* **1984**, *104*, 2224.
(12) Teo, B. K.; Hong, M. C.; Zhang, H.; Huang, D. B. *Angew. Chem., Int. Ed. Engl.* **1987**, *26*, 897.
(13) Teo, B. K.; Zhang, H. *J. Cluster Sci.* **1990**, *1*, 155.
(14) Teo, B. K.; Zhang, H. *Proc. Natl. Acad. Sci. U.S.A.* **1991**, *88*, 5067.
(15) Teo, B. K.; Zhang, H. *Polyhedron* **1990**, *9*, 1985.
(16) Ozin, G. A.; Mitchell, S. A. *Angew. Chem., Int. Ed. Engl.* **1983**, *22*, 674 and references therein.
(17) Ozin, G. A.; Huber, H. *Inorg. Chem.* **1978**, *17*, 155.
(18) Howard, J. A.; Preston, K. F.; Sutcliffe, R.; Mile, B.; Tse, J. S. *J. Phys. Chem.* **1983**, *87*, 2268.
(19) Howard, J. A.; Preston, K. F.; Mile, B. *J. Am. Chem. Soc.* **1981**, *103*, 6226.
(20) Kim, Y.; Seff, K. *J. Am. Chem. Soc.* **1977**, *99*, 7055.
(21) Michalik, J.; Wasowicz, T.; Van der Pol, A.; Reijerse, E. J.; De Boer, E.; *J. Chem. Soc., Chem. Commun.* **1992**, 29.
(22) Tani, T. *Physics Today* **1989**, *September*, 36.
(23) Farmery, K.; Kilner, M.; Greatrex, R.; Greenwood, N. N. *J. Chem. Soc. Sect. A* **1969**, 2339.
(24) Kruzic, P. J.; San Filippo, J.; Hutchinson, B.; Hance, R. L.; Daniels, L. M. *J. Am. Chem. Soc.* **1981**, *103*, 2129.

0002-7863/92/1514-5708$03.00/0

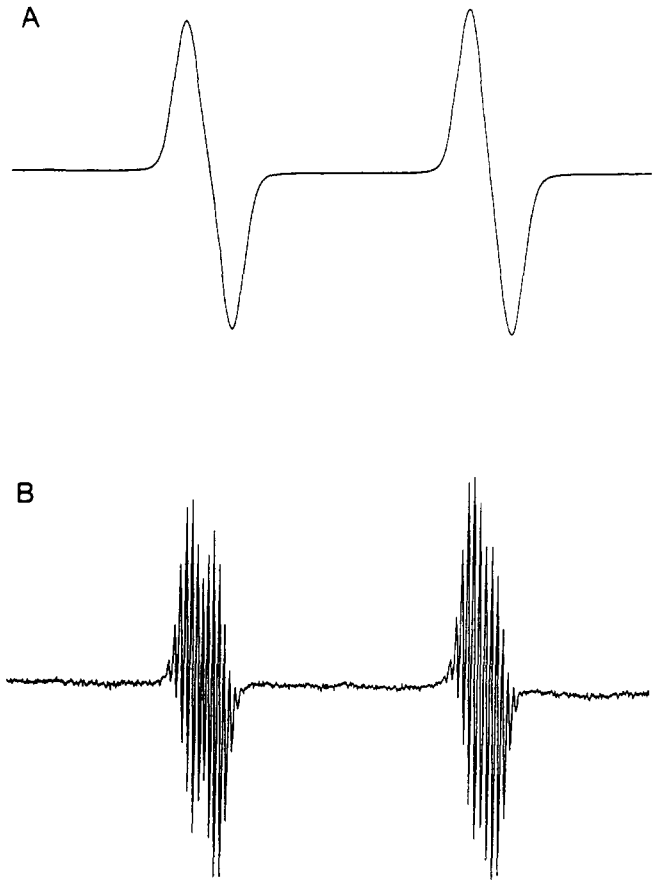

Figure 1. ESR spectrum at 300 K of $[NMe_3CH_2Ph]_4[Ag_{13}Fe_8(CO)_{32}]$ as a powdered crystalline sample (A) and in acetonitrile solution containing ca. 10% of benzene (B).

absorptions at 1980 and 1890 cm^{-1}. The suspension is filtered to eliminate some silver metal, and the solution is evaporated under vacuum. After metathesis of the residue in methanol with tetrasubstituted ammonium or phosphonium salts, the resulting precipitate is washed with several portions of water and THF and extracted with acetonitrile. Crystallization by slow diffusion of twice an amount of diisopropyl ether affords well-shaped black crystals in 40–70% yields. These have been shown by X-ray crystallography, ESR spectroscopy, and elemental analyses to consist of salts of the new $[Ag_{13}Fe_8(CO)_{32}]^{4-}$ tetraanion. The $[NEt_4]^+$, $[N(CH_3)_3CH_2Ph]^+$, and $[(PPh_3)_2N]^+$ salts of $[Ag_{13}Fe_8(CO)_{32}]^{4-}$ are soluble in acetone and acetonitrile, in which they give orange-brown solutions showing carbonyl infrared absorptions at 1980 (s) and 1890 (m) cm^{-1}. The ESR spectrum of a solid powdered sample of $[N(CH_3)_3CH_2Ph]_4[Ag_{13}Fe_8(CO)_{32}]$ at room temperature is shown in Figure 1A and essentially consists of a doublet (g = 1.9937) with a ca. 170.5 G splitting. In contrast, this same salt in acetonitrile solution containing ca. 10% benzene displays the hyperfine structure shown in Figure 1B. As shown in Figure 2, where the experimental (A) and simulated (B) spectra are compared, the ESR pattern of $[Ag_{13}Fe_8(CO)_{32}]^{4-}$ in acetonitrile can be simulated perfectly by computer on assuming that it consists of two almost equally intense doublets centered at g = 1.9937 and g = 1.9931 with coupling constants of 183.5 and 159 G, respectively; each line of the two doublets being split further into 13 lines with a unique coupling constant of 3.5 G. Since the naturally occurring isotopic mixture of silver consists of two isotopes, that is ^{107}Ag (51.35% natural abundance, $S = {}^1/_2$, μ = −0.1130) and ^{109}Ag (48.65% natural abundance, $S = {}^1/_2$, μ = −0.1299), the doublet with the greatest coupling constant should be associated with the $[^{107}Ag_{12-x}{}^{109}Ag_x(\mu_{12}\text{-}{}^{109}Ag)Fe_8(CO)_{32}]^{4-}$ set of isotopomers and should arise from the coupling of the unpaired electron with the unique interstitial ^{109}Ag atom. Conversely, the second doublet with a slightly inferior coupling constant is due to the second $[^{107}Ag_{12-x}{}^{109}Ag_x(\mu_{12}\text{-}{}^{107}Ag)Fe_8(CO)_{32}]^{4-}$ set

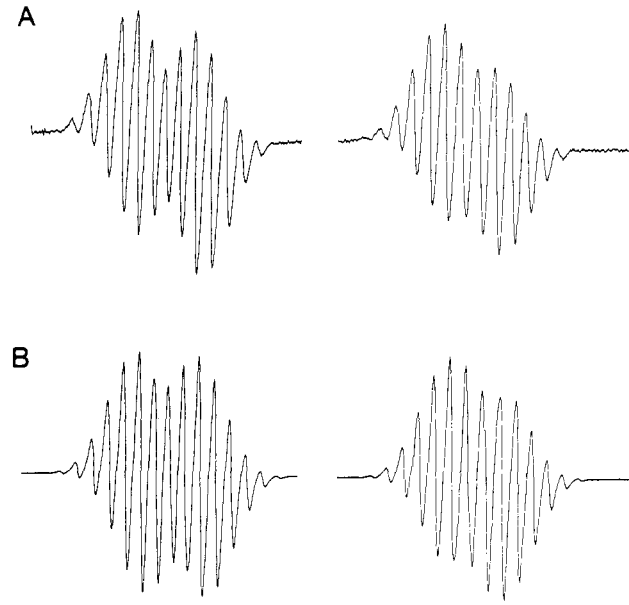

Figure 2. Experimental (A) and simulated (B) ESR solution spectra of $[NMe_3CH_2Ph]_4[Ag_{13}Fe_8(CO)_{32}]$.

of isotopomers. The observed $A(^{109}Ag)/A(^{107}Ag)$ ratio of 1.154 matches the corresponding ratio measured in silver atoms isolated in noble gas matrices[25] and corresponds well to the ratio of the magnetic moments of the two silver isotopes. A difference of ca. 13% in the greater coupling constant of the two isotopes justifies the deceptively simple ESR spectrum shown by the above mixture of isotopomers; indeed, further splitting of each doublet line by hyperfine coupling with the 12 peripheral silver atoms probably only gives rise to 13 observable lines with an apparent coupling constant of 3.5 G because the difference in the ^{109}Ag and ^{107}Ag coupling constants of the peripheral atoms is too small, and the two isotopes behave as if they are equivalent. The significant difference between the coupling constants of the interstitial and the peripheral silver atoms indicates that the unpaired electron is mainly associated with the interstitial silver atom and probably resides in a nonbonding or weakly antibonding molecular orbitals of the Ag_{13} metal core. Using the suggested one-electron parameter of ^{107}Ag,[26] the observed coupling constants point out a spin population of 0.25 for the interstitial and less than 0.01 for the peripheral ^{107}Ag 5s orbitals.

2. The Molecular Structure of $[Ag_{12}(\mu_{12}\text{-}Ag)\{Fe(CO)_4\}_8]^{4-}$. The crystals of the title anion contain discrete anions placed at inversion centers and $[N(PPh_3)_2]^+$ cations in general positions. Two molecules of clathrated acetone per anion are also present. Relevant bond distances and angles are listed in Table I.

As shown in Figure 4, the $[Ag_{12}(\mu_{12}\text{-}Ag)\{Fe(CO)_4\}_8]^{4-}$ anion contains a centered cuboctahedron of silver atoms, i.e., a fragment of the cubic face centered structure of the bulk metal. All the triangular faces of the cuboctahedron are capped by $Fe(CO)_4$ fragments adopting C_{3v} ligand arrangement. Quite exceptionally for a high nuclearity cluster the CO ligand geometry conforms to the O_h idealized symmetry of the metal atom core. The Fe atoms, on the other hand, do not make an extension of the close packing of Ag atoms and define instead a distorted cube. For this reason, the $Fe(CO)_4$ groups can be considered as nonconventional ligands of the Ag_{13} cluster. In spite of the potentially high symmetry of the isolated anion only the inversion center is retained in the crystal. This descends not only from the stoichiometry of the salt and factors of packing efficiency but also from the ligand crowding on the cluster surface. An inspection of the Fe–Ag distances [av 2.737, range 2.695–2.772 (1) Å] shows that all of the $Fe(CO)_4$ groups have some degree of distortion. There is also an equivalent degree of asymmetry present in the

(25) Kasai, P. H.; McLeod, D., Jr. *J. Chem. Phys.* **1971**, *55*, 1566.
(26) Morton, R. J.; Preston, K. F. *J. Magn. Reson.* **1978**, *30*, 577.

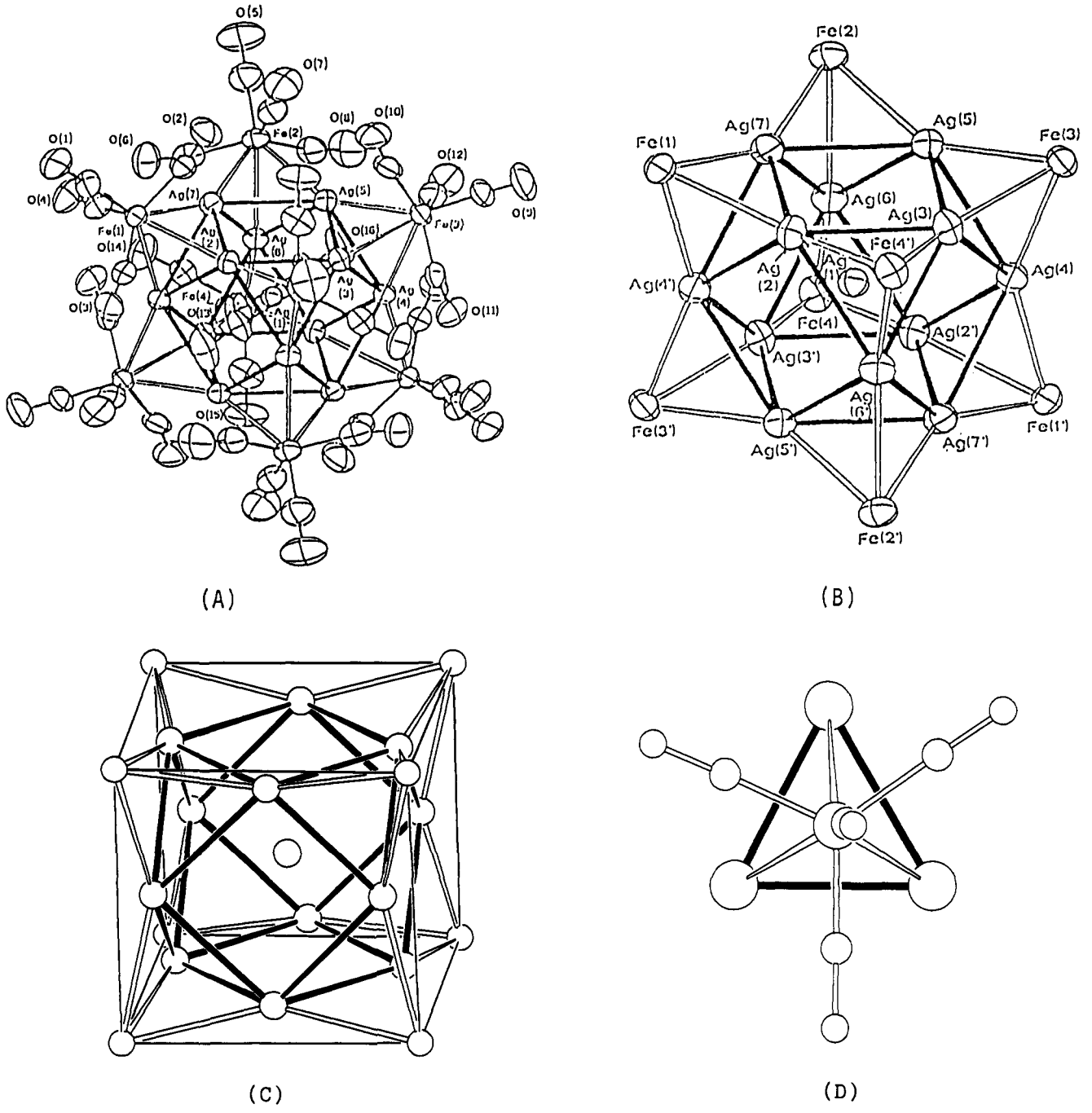

Figure 3. (A) ORTEP drawing of the $[Ag_{12}(\mu_{12}\text{-}Ag)\{Fe(CO)_4\}_8]^{4-}$ tetraanion showing the atomic numbering scheme. Ag(1) is on a crystallographic center of inversion which relates each unlabeled atom to a labeled one. The carbon atoms of the CO groups bear the same numbering as the oxygen atoms. Thermal ellipsoids are drawn at 50% probability. (B) View of the $Ag_{13}Fe_8$ cluster core showing its idealized O_h symmetry. (C) Schematic drawing displaying the overall cubic shape of the metal atom cluster. (D) Coordination around the iron atom in the $Ag_3Fe(CO)_4$ fragments.

nonbonding interactions [av axial–equatorial C···C contacts 2.52, range 2.46–2.56 Å]. Axial and equatorial CO ligands show different Fe–C, C–O, distances and Fe–C–O angles: 1.74, 1.16 Å, 178° and 1.79, 1.15 Å, 169°, respectively. It is worth noting the bending of the equatorial ligands indicative of weak bonding interactions with the Ag atoms [av Ag···C contacts 2.75 Å]. The mean value of the Ag–Fe distances can be compared to the corresponding value in $[Ag_6\{Fe(CO)_4\}_3\{(Ph_2P)_3CH\}]$, 2.69 Å.[7]

The inner Ag_{13} core looks so compact and symmetric that one would hardly expect significant deviations from its idealized O_h symmetry. However, the dispersion of the Ag–Ag distances is more than significant, in particular for the surface edges. The center–surface distances are as follows: av 2.923, range 2.882–3.001 (1) Å. The surface–surface distances exhibit the following values: av 2.923, range 2.826–3.106 (1) Å. The mean values compare well with the Ag–Ag distance in the metal 2.89 and in the previously cited Ag_6 cluster, 2.91. As for the Ag–Fe distances, the anionic charge accounts for the slight differences noted. The deformations in the Ag_{13} polyhedron do not follow a well recognizable pattern. The maximum regularity that can be envisaged is a 2-fold symmetry around the Ag(2)–Ag(1)–Ag(2′) axis. The coincidence of the average values for the center–surface and surface–surface distances and the greater dispersion of the latter indicate that the polyhedron is quite soft, and the deformations are generated from the ligand–ligand contacts and interion interactions.

The clusters of closest similarity with which comparisons of rigidity are possible are the anticuboctahedral polyhedra in $[Rh_{13}H(CO)_{24}]^{4-}$[27] and $[Rh_{12}Pt(CO)_{24}]^{4-}$,[28] in which the range

(27) Ciani, G.; Sironi, A.; Martinengo, S. *J. Chem. Soc., Dalton Trans.* **1981**, 519.

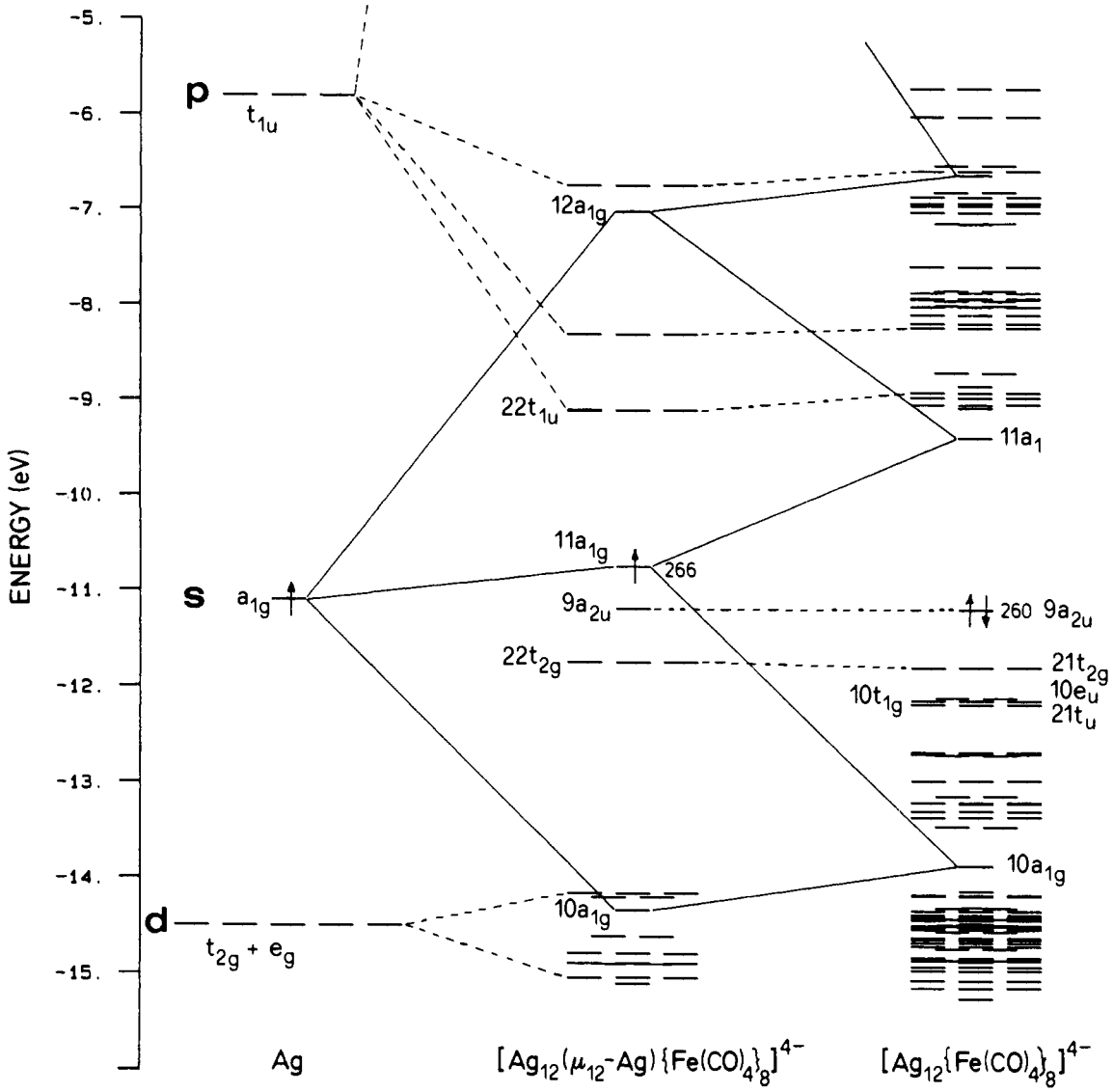

Figure 4. Interaction diagram between the inner Ag and the $[Ag_{12}\{Fe(CO)_4\}_8]^{n-}$ to afford the $[Ag_{12}(\mu_{12}\text{-}Ag)\{Fe(CO)_4\}_8]^{n-}$ cluster. The $[Ag_{12}\{Fe(CO)_4\}_8]^{n-}$ energy levels are fully reported, whereas, in the case of the $[Ag_{12}(\mu_{12}\text{-}Ag)\{Fe(CO)_4\}_8]^{n-}$ cluster, only the frontier orbitals plus those containing a significant μ_{12}-Ag contribution are drawn. The reported electron occupation refers to $n = 4$.

Table I. Selected Bond Lengths (Å) and Angles (deg) for $[Ag_{13}Fe_8(CO)_{32}]^{4-}$

Ag(1)–Ag(2)	3.001 (1)	Fe(1)–Ag(7)	2.762 (1)
Ag(1)–Ag(3)	2.904 (1)	Fe(1)–Ag(2)	2.705 (1)
Ag(1)–Ag(4)	2.899 (1)	Fe(1)–Ag(4′)	2.753 (1)
Ag(1)–Ag(5)	2.882 (1)	Fe(2)–Ag(5)	2.749 (1)
Ag(1)–Ag(6)	2.938 (1)	Fe(2)–Ag(6)	2.712 (1)
Ag(1)–Ag(7)	2.918 (1)	Fe(2)–Ag(7)	2.744 (1)
Ag(2)–Ag(3)	2.826 (1)	Fe(3)–Ag(3)	2.695 (1)
Ag(2)–Ag(7)	2.955 (1)	Fe(3)–Ag(4)	2.727 (1)
Ag(2)–Ag(4′)	2.867 (1)	Fe(3)–Ag(5)	2.735 (1)
Ag(2)–Ag(6′)	2.903 (1)	Fe–C(ax)	1.74 (av)
Ag(3)–Ag(4)	3.106 (1)	C–O(ax)	1.16 (av)
Ag(3)–Ag(5)	2.940 (1)	Fe–C(eq)	1.79 (av)
Ag(3)–Ag(6′)	2.851 (1)	C–O(eq)	1.15 (av)
Ag(4)–Ag(5)	2.907 (1)	Fe–C–O(ax)	178 (av)
Ag(5)–Ag(6)	2.933 (1)	Fe–C–O(eq)	169 (av)
Ag(5)–Ag(7)	2.914 (1)	Ag···C(eq)	2.75 (av)
Ag(6)–Ag(7)	2.999 (1)	C(ax)···C(eq)	2.52 (av)
Ag(4′)–Ag(7)	2.880 (1)		

of the metal–metal distances is much narrower (2.782, range 2.718–2.870 (3) and 2.778, range 2.713–2.849 (7) Å, respectively), in spite of the lower symmetry of the ligand–core interactions. The shorter average bond distances in the Rh_{13} and $Rh_{12}Pt$ polyhedra with respect to Ag_{13} indicate higher bond order in the former and justify the greater toughness of the anticuboctahedral clusters.

3. Bonding Analysis of $[Ag_{13}Fe_8(CO)_{32}]^{4-}$. Cuboctahedral clusters are rare, and at present the only known species displaying such a geometry of metal atoms are $Pt_{15}(CO)_8H_8(PBu^t_3)_6$, A,[29] which has a Pt-filled Pt_{12} cuboctahedral core and 162 cluster valence electrons (CVE), and $[Cu_{12}S_8]^{4-}$, B,[30] which has an empty Cu_{12} cage and 168 CVE. Rh- and Pt-filled anticuboctahedral Rh_{12} cores have been found in the 170 CVE $[Rh_{13}(CO)_{24}H_{5-n}]^{n-}$ and $[Rh_{12}Pt(CO)_{24}]^{4-}$ clusters, C.[27,28] All these clusters show different CVE numbers which in the case of A have been justified with the polyhedral skeletal electron pair theory (PSEPT) for *porcupine* clusters,[31] in the case of B with the effective atomic number (EAN) rule,[33] and with PSEPT for four-connected polyhedral clusters in the case of C.[34]

(28) Fumagalli, A.; Martinengo, S.; Ciani, G. *J. Chem. Soc., Chem. Commun.* **1983**, 1381.

(29) Howard, J. A. K.; Spencer, J. L.; Turner, D. G. *J. Chem. Soc., Dalton Trans.* **1987**, 259.

(30) Betz, P.; Krebs, B.; Henkel, G. *Angew. Chem., Int. Ed. Engl.* **1984**, *23*, 311.

(31) High nuclearity clusters where radial bonding predominates are characterized by a total of $(12m_s + \Delta_i)$ CVE, that is 162 CVE in the present case ($m_s = 12$, $\Delta_i = 18$); rule 7 in ref 32.

(32) Mingos, D. M. P.; May, A. S. In *Chemistry of Metal Cluster Complexes*; Shriver, D. S., Kaesz, H. D., Adams, R. D., Eds.; VCH: 1990.

(33) According to the EAN rule a cuboctahedral cage, having 12 vertices and 24 edges, should be stable with 12 × 18–24 × 2 = 168 CVE.

The electron count of the $[Ag_{12}(\mu_{12}\text{-}Ag)\{Fe(CO)_4\}_8]^{4-}$ anion depends on the model assumed for the nuclearity of the cluster. If the iron atoms are considered as part of the cluster, the octacapped $Ag_{13}Fe_8$ cuboctahedron would have 275 CVE. Alternatively, the title compound may be considered as a cuboctahedral Ag_{13} cluster, with 179 CVE, stabilized by eight four-electron donor $Fe(CO)_4$ ligands.[35] The two points of view are equivalent and consistently show the presence of nine electrons in excess on the PSEPT expectations for the two different polyhedra;[36] therefore, in the following discussion we will refer only to the second point of view.

It is worth noting that, under the assumption that the $Fe(CO)_4$ fragment is a two-electron donor (which is however inadequate in the present case),[35] the Ag_{13}^{4-} cuboctahedron would turn out to be electron short by formally achieving 163 CVE, but would be isoelectronic with the icosahedral $[Au_{13}(dppm)_6]^{4+}$,[37] and would have one electron more than the Pt_{13} cuboctahedron found in $Pt_{15}(CO)_8H_8(PBu^t_3)_6$[29] as well as the icosahedral $[Au_{13}(PPhMe_2)_{10}Cl_2]^{3+}$.[38]

The observed CVE value (179) could be related to that expected by the PSEPT approach (170 CVE) assuming that the extra nine electrons derive from the presence of a filled d shell of the interstitial Ag atom, which does not significantly interact with the cage orbitals and which can be dismissed in the electron count. A similar feature has been recently observed in the icosahedral $[Ni_{10}Sb_2(\mu_{12}\text{-}Ni)(CO)_{18}\{Ni(CO)_3\}_2]^{n-}$ and $[Ni_{10}Bi_2(\mu_{12}\text{-}Ni)(CO)_{18}]^{n-}$ (n = 2–4),[39,40] which also have 8, 9, and 10 CVE in excess with respect to PSEPT predictions. Accordingly, if the $4d^{10}$ shell is considered inner core for all the silver atoms, the Ag_{13}^{4-} cuboctahedral moiety stabilized by the eight four-electron donor $Fe(CO)_4$ groups would possess 49 CVE, one less than the icosahedral $B_{12}H_{12}^{2-}$.[41]

However, why the unfilled Cu_{12} and the filled Ag_{13} cuboctahedral cluster cores differ in their electron counts by 11 electrons (eventually 12 in a corresponding even-electron $[Ag_{13}Fe_8(CO)_{32}]^{5-}$) still has to be explained. A difference of ten electrons could be accounted for by considering the 4d filled shell of the interstitial silver atom as inert, but a greater difference seems to challenge the well documented rule that centered and noncentered clusters require the same number of skeletal electron pairs.[42] In order to verify the above discrepancy and to explain the ESR features of $[Ag_{13}Fe_8(CO)_{32}]^{4-}$, extended Huckel (EH) calculations[43–45] on idealized noncentered and Ag-centered Ag_{12} cuboctahedra have been carried out. The bare cluster approach,[46] however, fails to foresee the correct bonding capabilities of the two metal clusters by predicting 176 and 186 CVE for species based on Ag_{12} and Ag_{13} metal cores, respectively (Figure S1 of the supplementary material). On the contrary, EH computations on the whole, ligand covered clusters (see Figure 5)[47] clearly show that the MO level

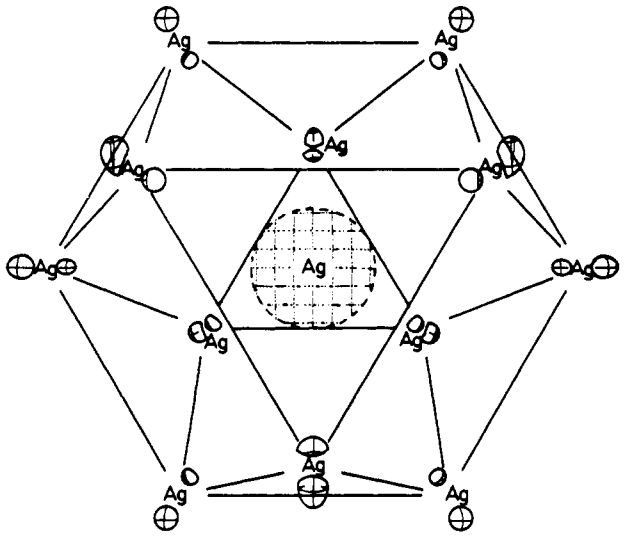

Figure 5. CACAO[53] plot of the SOMO of $[Ag_{12}(\mu_{12}\text{-}Ag)\{Fe(CO)_4\}_8]^{4-}$ representing the atomic orbital composition on each metal center. The picture concerns the Ag_{13} core along because only the Ag atoms are magnetically active. The peripheral Ag atom contributions are all equivalent because of the A_{1g} symmetry and are significantly smaller than that of the μ_{12}-Ag atom.

pattern for $[Ag_{12}\{Fe(CO)_4\}_8]^{n-}$ has a candidate HOMO–LUMO gap above the orbital 260, while this is present only above the orbital 266 in $[Ag_{12}(\mu_{12}\text{-}Ag)\{Fe(CO)_4\}_8]^{n-}$. In the case of $[Ag_{12}\{Fe(CO)_4\}_8]^{n-}$, 260 × 2 valence electrons are attained for n = 4, and the hypothetical $[Ag_{12}\{Fe(CO)_4\}_8]^{4-}$ species would have 168 CVE, *as expected on the basis of the EAN rule*, and would be isoelectronic with $[Cu_{12}S_8]^{4-}$.[50] In the case of $[Ag_{12}(\mu_{12}\text{-}Ag)\{Fe(CO)_4\}_8]^{n-}$, 266 × 2 valence electrons are attained for n = 5, and the corresponding species would have 180 CVE, i.e., 12 extra CVE with respect to the unfilled cluster.

The different electron bookkeeping for the two species is simply accounted for by the unability of μ_{12}-Ag d and s orbitals to afford the corresponding empty antibonding orbitals upon interaction with the $[Ag_{12}\{Fe(CO)_4\}_8]^{4-}$ fragment. In fact, the interaction diagram[51,52] between the inner Ag and the empty cluster (Figure 5) clearly shows that the μ_{12}-Ag d orbitals contribute to a narrow band of filled orbitals, because of their relative low energy and of the small ⟨d|cage⟩ group overlaps, and, the μ_{12}-Ag s orbital, being the intermediate term of a three orbital interaction, correlates with a low energy nonbonding orbital (the HOMO) in spite of the large ⟨s|cage⟩ group overlaps.

Depending on the occupancy of the aforementioned nonbonding orbital the filled cluster has 10–12 CVE more than the unfilled; in the case of the paramagnetic $[Ag_{12}(\mu_{12}\text{-}Ag)\{Fe(CO)_4\}_8]^{4-}$ species the HOMO is singly occupied and its composition (Figure 5) can be qualitatively related to the hyperfine splittings observed in the ESR spectrum which shows a stronger coupling of the unpaired electron with the inner silver atom and looser coupling with the outer 12 silver atoms. Hyperfine coupling constants depend on

(34) Rule 3 in ref 32 states that four-connected polyhedral molecules are characterized by a total of $14m_s + 2$ CVE, that is 170 CVE in the present case (m_s = 12).

(35) The $Fe(CO)_4$ fragments in $[Ag_{12}(\mu_{12}\text{-}Ag)\{Fe(CO)_4\}_8]^{4-}$ display an axially-vacant trigonal-bipyramidal geometry. The adoption of a local C_{3v} symmetry leads to a $Fe(CO)_4$ fragment with a doubly degenerate HOMO level and a low energy LUMO; this implies that the $Fe(CO)_4$ trigonal-pyramidal C_{3v} fragment may behave both as a Lewis acid or as a formal four-electron ligand.

(36) An octacapped cuboctahedron should have 170 + 8 × 12 = 266 CVE.

(37) Van der Welden, J. W. A.; Vollenbroek, F. A.; Boer, J. J.; Beurskens, P. T.; Smits, J. M. M.; Bosman, W. P. *Rec. J. R. Neth. Chem. Soc.* **1981**, *100*, 148.

(38) Briant, C. E.; Theobald, B. R. C.; White, J. W.; Bell, L. K.; Mingos, D. M. P. *J. Chem. Soc., Chem. Commun.* **1981**, 201.

(39) Albano, V. G.; Demartin, F.; Iapalucci, M. C.; Laschi, F.; Longoni, G.; Sironi, A.; Zanello, P. *J. Chem. Soc., Dalton Trans.* **1991**, 739.

(40) Albano, V. G.; Demartin, F.; Iapalucci, M. C.; Longoni, G.; Monari, M.; Zanello, P. *J. Chem. Soc., Dalton Trans.*, in press.

(41) Muetterties, E. L. *Boron Hydride Chemistry*; Academic Press: New York, 1975.

(42) Mingos, D. M. P.; Zheniang, L. *J. Chem. Soc., Dalton Trans.* **1988**, 1657.

(43) Hoffmann, R. *J. Chem. Phys.* **1963**, *39*, 1397.

(44) Hoffmann, R.; Lipscomb, W. N. *J. Chem. Phys.* **1962**, *36*, 3489.

(45) Hoffmann, R.; Lipscomb, W. N. *J. Chem. Phys.* **1962**, *37*, 2872.

(46) Lahuer, J. W. *J. Am. Chem. Soc.* **1978**, *100*, 5305.

(47) Molecular geometries have been obtained using a molecular mechanics program capable of handling metal carbonyl clusters,[48] assuming O_h symmetry and the following bonding parameters: Ag–Ag = 2.923, Ag–Fe = 2.737, Fe–C_{eq} = 1.79, Fe–C_{ax} = 1.74, and C–O = 1.15 Å. The EHT parameters for Ag have been taken from ref 49.

(48) Sironi, A. *Inorg. Chem.*, submitted.

(49) Jorgensen, K. A.; Hoffmann, R. *J. Phys. Chem.* **1990**, *94*, 3046.

(50) The $[Ag_m\{Fe(CO)_4\}_8]^{n-}$ – $[Cu_mS_8]^{n-}$ (m = 12, 13) relationship is not casual. They have a markedly similar stereochemistry (a cuboctahedron of either silver or copper atoms capped by 8 μ_3 ligands); the $Fe(CO)_4$ and S ligands are isolobal, and the MO level patterns of the Cu_{12}/Ag_{12} and Cu_{13}/Ag_{13} couples, which are reported in Figure S1 of the supplementary material, are rather similar even if the shorter Ag–Ag interactions, with respect to the metal–metal distances in the bulk metal, make the Ag_m patterns more spread out.

(51) Hoffmann, R.; Fujimoto, H.; Svenson, J. R.; Wan, C. C. *J. Am. Chem. Soc.* **1973**, *95*, 7644.

(52) Hoffmann, R.; Fujimoto, H. *J. Phys. Chem.* **1974**, *78*, 1167.

Table II. Crystal Data and Experimental Details for $[N(PPh_3)_2]_4[Ag_{13}Fe_8(CO)_{32}]\cdot 2(CH_3)_2CO$

complex	$[N(PPh_3)_2]_4[Ag_{13}Fe_8(CO)_{32}]\cdot 2(CH_3)_2CO$
formula	$C_{176}H_{120}Ag_{13}Fe_8N_4O_{32}P_8\cdot 2C_3H_6O$
M	5015.9
crystal size, mm	0.125 × 0.20 × 0.40
system	monoclinic
space group	$P2_1/n$
a, Å	18.321 (2)
b, Å	22.429 (3)
c, Å	22.150 (1)
β, deg	92.24 (2)
V, Å^3	9095.0
Z	2
D_c, g/cm^3	1.83
$F(000)$	4926
radiation (graphite monochromated) (λ, Å)	Mo Kα (0.71067)
μ(Mo Kα), cm^{-1}	21.0
diffractometer	Enraf-Nonius CAD-4
scan mode	ω
ϑ limits, deg	3–25
ω scan width, deg	1.20 + 0.35tgϑ
prescan rate, deg min^{-1}	4
prescan acceptance $\sigma(I)/I$	1.00
required $\sigma(I)/I$	0.01
max. scan time, s	90
standard reflcns	3 remeasured periodically no decay
reflcns collected	12526
unique obsd reflcns $[F_o > 4\sigma(F_o)]$	9269
no. of refined parameters	600
R,[a] R_w[b]	0.0410, 0.0426
K, g[c]	1.389, 0.0001
quality-of-fit indicator[d]	1.65

[a] $R = \sum||F_o| - |F_c||/\sum|F_o|$. [b] $R_w = \sum(|F_o| - |F_c|)w^{1/2}/\sum w^{1/2}|F_o|$. [c] $w = K/[\sigma^2(F) + |g|F^2]$. [d] Quality-of-fit = $[\sum w(|F_o| - |F_c|)^2/(N_{obs} - N_{par})]^{1/2}$.

the electron spin density at the nuclei: the larger the coefficient on the singly occupied MO, the larger the coupling constant. The s orbitals are the only ones directly affording nonzero spin density on the nucleus but, because of spin polarization, the p and d contributions are also important. As shown in Figure 5, the semioccupied molecular orbital (SOMO) is essentially nonbonding with respect to the Ag_{inner}–Ag_{outer} interaction and has a large amount of character from the 5s orbital of the interstitial silver atom.

Conclusion

The molecular structure of the $[Ag_{12}(\mu_{12}\text{-}Ag)\{Fe(CO)_4\}_8]^{4-}$ tetraanion shows that the eight μ_3-capping $Fe(CO)_4$ groups are somewhat crowded. As shown by computer simulation, the conversion of the inner cuboctahedron into either an anticuboctahedron or an icosahedron results in an unavoidable crash of carbonyl groups. It appears, therefore, reasonable to conclude that adoption of a cuboctahedral stereogeometry by the inner Ag_{13} metal core is dictated by steric reasons and that the packing of the ligands may determine the geometry of the inner metal core.

Besides, as shown by the interaction diagram of Figure 5 (the qualitative validity of which is nicely supported by the experimental ESR spectrum), it is confirmed not only that interstitial transition elements can alter the cluster electron count when having contracted low energy d orbitals but also that even the strongly interacting s orbital can ultimately afford a low energy filled orbital when its energy is in between the HOMO–LUMO gap of the empty cluster. This points out a further important effect of the outer ligand geometry; it controls the shape and the relative energy of the empty cluster orbitals, tunes the HOMO–LUMO gap, and allows for the presence of a low energy unoccupied orbital (in the present case the LUMO) stabilizing the s orbital of the interstitial atom.

Finally, the reported EH calculations suggest that $[Ag_{12}(\mu_{12}\text{-}Ag)\{Fe(CO)_4\}_8]^{n-}$ species with $n = 3$ and 5 could be sufficiently stable to be isolated and characterized; attempts in this direction are in progress.

Experimental Section

All reactions including sample manipulations were carried out with standard Schlenk techniques under nitrogen in dried solvents. The $[Fe(CO)_4]^{2-}$ salts were prepared according to literature methods.[54] Analyses of Fe and Ag have been performed by atomic absorption on a Pye-Unicam instrument and gravimetrically as BPh_4^- salts for the tetrasubstituted ammonium cations. Infrared spectra were recorded on a Perkin Elmer 257 grating spectrophotometer using CaF_2 cells. Proton NMR spectra were recorded on a Bruker WP-200 spectrometer. The ESR measurements have been carried out on a Varian E-104 instrument on using diphenylpicrylhydrazil as reference.

1. Synthesis of $[NEt_4]_4[Ag_{13}Fe_8(CO)_{32}]$. A solution of $AgBF_4$ (2.4 g) in THF (50 mL) was added in portions (5 mL) to a stirred suspension of $Na_2[Fe(CO)_4]\cdot x$THF (2.51 g, 7.8 mmol for $x = 1.5$) in THF (40 mL) over 2 h. The resulting dark suspension was evaporated in vacuum to dryness, and the residue was suspended in methanol (100 mL) and filtered. The methanol solution was precipitated by addition of solid NEt_4Br. The resulting solid material was washed several times with water and THF. The remaining precipitate was dissolved in acetone (40 mL) and precipitated by slow diffusion of isopropyl alcohol (80 mL) to give 1.57 g of well-shaped black crystals of $[NEt_4]_4[Ag_{13}Fe_8(CO)_{32}]$. These are soluble in acetone and acetonitrile, less soluble in THF, and insoluble in nonpolar solvents. Anal. Calcd for $[NEt_4]_4[Ag_{13}Fe_8(CO)_{32}]$: NEt_4^+, 15.94; Ag, 42.95; Fe, 13.68. Found: NEt_4^+, 15.1; Ag, 41.6; Fe, 13.2.

The corresponding $[NMe_3CH_2Ph]^+$ and $[N(PPh_3)_2]^+$ salts have been similarly prepared and crystallized either from acetone–isopropyl alcohol or acetonitrile–diisopropyl ether.

2. X-ray Structure Determination of $[N(PPh_3)_2]_4[Ag_{13}Fe_8(CO)_{32}]\cdot 2(CH_3)_2CO$. Crystal data and details of the data collection are given in Table II. The diffraction intensities were collected on an Enraf-Nonius CAD-4 diffractometer, and the cell constants were determined from a list of reflections found by an automated search routine. Data were corrected for Lorentz and polarization effects. No decay correction was necessary. All calculations were performed using the SHELX-76 system of programs.[55] The metal atom positions were determined by direct methods and all non-hydrogen atoms located from Fourier difference syntheses. The anions were located around inversion centers, while two independent cations and one clathrated acetone molecule were found in general positions. An empirical absorption correction was applied by using the Walker and Stuart method[56] once the structural model was completely defined and all atoms refined isotropically. The phenyl rings of the cations were treated as rigid groups of idealized geometry (C–C distance 1.395 Å, C–C–C 120°). Hydrogen atoms were added in calculated positions (d_{CH} = 1.08 Å), and their positions were not refined but continuously updated with respect to their carbon atoms. The final refinement of positional and thermal parameters proceeded using anisotropic thermal parameters for all atoms except the phenyl C atoms and the acetone molecule. The final difference Fourier map showed peaks not exceeding 1.0 eÅ^{-3}. Final positional parameters with their estimated standard deviations corresponding to the final least-squares refinement cycles are given in the supplementary material (Table S1).

Acknowledgment. We thank the EEC (Contract ST2J-0479-C) and the MURST for a grant.

Supplementary Material Available: Tables of positional parameters (Table S1), calculated hydrogen atom coordinates (Table S2), anisotropic thermal parameters (Table S3), complete bond lengths and angles for $[N(PPh_3)_2]_4[Ag_{13}Fe_8(CO)_{32}]\cdot 2(CH_3)_2CO$ (Table S4), and MO level diagram for the Cu_{12}, Ag_{12}, Cu_{13}, and Ag_{13} bare clusters (Figure S1) (63 pages); listing of observed and calculated structure factors amplitudes used in the refinement for $[N(PPh_3)_2]_4[Ag_{13}Fe_8(CO)_{32}]\cdot 2(CH_3)_2CO$ (Table S5) (55 pages). Ordering information is given on any current masthead page.

(53) Mealli, C.; Proserpio, D. M. *J. Chem. Educ.* **1990**, *66*, 399.
(54) Collman, J. P.; Finke, R. G.; Cawse, J. N.; Brauman, J. I. *J. Am. Chem. Soc.* **1977**, *99*, 2515.
(55) Sheldrick, G. M. SHELX 76; System of computer programs; University of Cambridge: 1976.
(56) Walker, N.; Stuart, D. *Acta Crystallogr., Sect. A* **1983**, *39*, 158.